JOURNAL OF APPLIED POLYMER SCIENCE VOL. 7, PP. 643–665 (1963)

Peel Adhesion. II. A Theoretical Analysis*

JOHN L. GARDON, *Textile Research Laboratory, Rohm and Haas Co., Philadelphia, Pennsylvania*

In the preceding paper, referred to hereafter as Part I, peel test results obtained with acrylic binders on a cellophane substrate are discussed. Two of these binders gave the results that at low peeling rates peeling force increased with rate and the failure was cohesive, while at high peeling rates the force was rate independent and the failure was adhesive. At a given rate the peeling force increased with thickness. The two binders which gave these results were Rhoplex HA-8, a self-crosslinking polymer, and Polymer 305-A, which is a copolymer of 99% ethyl acrylate and 1% acrylic acid.

In the present report the rate-independent adhesive failure data are discussed in terms of a newly developed theory. In this theory the dependence of the peeling force upon the thickness of the adhesive layer is expressed in terms of such parameters as the moduli of the substrate and the binder, the thickness of the subtrate, the width of the sample, and the maximum stress developed in the glue line at the failure point. In adhesive failure this maximum stress is equal to the adhesive bond strength. This theory is applicable to conditions where it can be assumed that the substrate and the binder behave as Hookean bodies and the failure stress is insensitive to rate effects. At high peeling rates these requirements are approximated even if the binder and the substrate are viscoelastic. It will be shown that at high peeling rates the rate of substrate and binder deformation is very high so that it is reasonable to expect that viscous deformation processes are suppressed and Hookean behavior is approached. It is also important that at these high rates adhesive failure occurs. If the adhesive bond is due to short range secondary valence forces, only small volume elements are displaced adjacent to the interface at failure. Thus rupturing would not be a viscous process but can be expected to occur instantaneously when the stress exceeds the adhesive bond strength. If these assumptions are correct, the effective adhesive bond strength is indeed insensitive to rate effects.

Because of the sensitivity of the peeling force to testing variables, a peel test at a constant rate and constant adhesive layer thickness is not an unequivocal measure of adhesiveness. However, the maximum adhesive

* This is part of a paper presented at the Annual Meeting of the Society of Rheology, Madison, Wisc., on October 31, 1961.

failure stress, which can be calculated from the adhesive layer thickness dependence of rate-independent peeling force, is a parameter which is independent of the testing variables and is a true measure of adhesiveness.

DERIVATION OF THE THEORY

The Model

Figure 1 shows a representation of the shape of the samples during peeling, based on photographs at 28-fold magnification. To take pictures slow peeling rates had to be employed. At low rates of peeling the rates of strain in the substrate and binder are low and their viscoelastic nature is

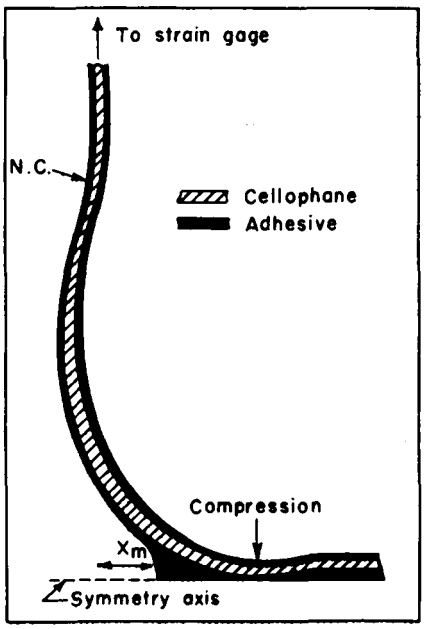

Fig. 1. Representation of the shape of the upper half of a test sample at steady-state peeling based on pictures taken on samples peeled at 0.02 to 0.1 in./min. cross-head speed and exhibiting cohesive failure. The negative curvature at point *N.C.* would not occur if the cellophane were really elastic; the bulging out of the cellophane beyond the axis of the force is due to its viscoelasticity. At force values higher than 300 g./in. this negative curvature is not apparent. The distance x_m between the force axis and the point of failure is the lower the greater the adhesive layer thickness (t_a) at a given force (F) or the higher is F at a given t_a.

predominant. Because of the viscous effects, the curved cellophane does not straighten out immediately when it becomes tangential to the plane of the peeling force. Instead, it bends out of this plane and subsequently bends back, so that at point N.C. negative curvature develops. Such negative curvature would not be found if viscous effects in the substrate were suppressed. In interpreting Figure 1 it should be borne in mind that

TABLE I

Variation of the Distance between Force Axis and Point of Failure (x_m) with the Thickness of the Adhesive Layer (t_a) and Peeling Forces (F) at Low Rates of Testing[a]

t_a (cm. $\times 10^4$)	154	42.7	10.0	1.4	1.1
F (dyne/cm. $\times 10^{-4}$)	15.0	6.24	2.54	1.12	9.4
x_m (cm. $\times 10^2$)	0	1.0	5.3	14.0	1.8

[a] The first four columns represent data obtained with Rhoplex HA-8. The data of the last column were obtained with Rhoplex HA-12, another thermoset acrylic polymer which is harder, stronger and which adheres better to cellophane than Rhoplex HA-8. The x_m values were determined from pictures described in Figure 1.

the present analysis is not applicable to low peeling rates because the viscous effects are not sufficiently suppressed and, as shown in Part I, the peeling force is rate dependent. In spite of this limitation, the distance between the force axis and the failure point, x_m, can be calculated by eq. 17c, presented below, and the calculated value is of the right order of magnitude. Such calculations can be based on data of Table I with adhesive layer thickness less than 10μ. As indicated in Table I, the pictures show that x_m decreases with increasing force and increasing adhesive layer thick-

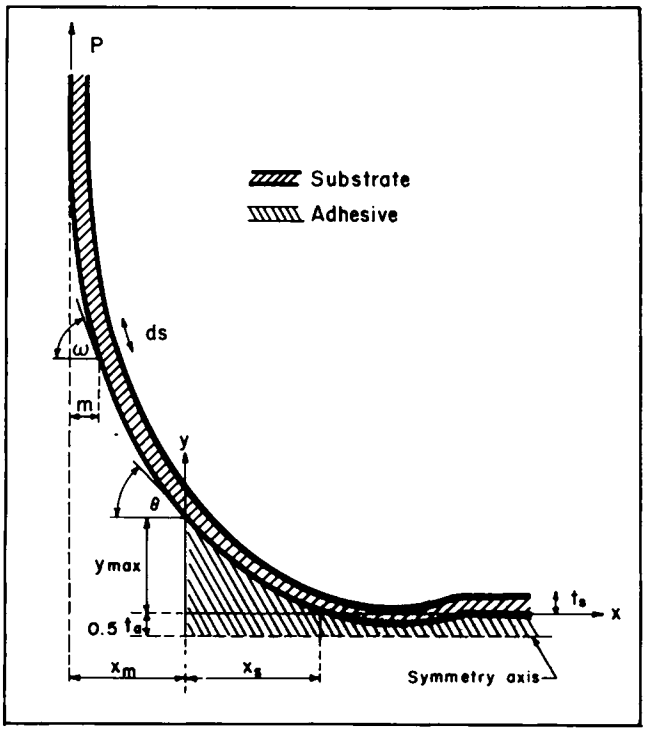

Fig. 2. The upper half of the model for the theoretical analysis or the peel adhesion

ness and that at very high values of peeling force and adhesive layer thickness, x_m vanishes and the force axis is at the point of failure. The photographs also indicate the existance of a compressive region within the glue line.

The upper half of the geometrical model used in the present analysis is shown in Figure 2. The following assumptions are made:

(*a*) Both the substrate and the adhesive are Hookean. It follows that there is no negative curvature in the unsupported portion of the substrate after failure.

(*b*) The modulus of the substrate is assumed to be much higher than that of the adhesive. This assumption justifies disregarding tensional elongation in the substrate; thus the only deformation in the substrate is bending. Furthermore, it follows from this assumption that the flexural rigidity of the substrate is not changed by the adhesive in contact with it.

(*c*) The stresses in the adhesive layer are calculated as if this layer consisted of an infinite number of independent vertical springs stretching between the two substrate films. It follows that the shear stresses and the tensional stresses in other than the vertical direction are disregarded and that the boundary of the adhesive layer at the point of rupture can be represented by a straight line.

(*d*) The sample is wide enough so that the edge effects can be disregarded and the problem can be handled in two-dimensional geometry.

(*e*) Equations that would hold for the neutral axis of the substrate are applicable to the substrate-adhesive interface and, after failure, to that surface of the substrate which had been glued to the other half of the sandwich. In line with this assumption, the axis of the peeling force runs not along the center of the substrate after the substrate has reached its vertical position but along its left surface as shown in Figure 2.

(*f*) The deflection of the substrate prior to rupture is low. This assumption is made for mathematical convenience.

(*g*) Failure occurs when the maximum stress in the adhesive layer exceeds the cohesive or adhesive strength.

(*h*) If adhesive failure occurs, the measured adhesive bond strength is independent of the slope angle of the adhesive-substrate interface at the point of failure.

(*i*) The strip extends to infinity in the positive x direction.

For the bending of the elastic substrate the Bernoulli-Euler law applies:

$$M = E_s I_s / r \tag{1}$$

where M is the bending moment and r is the radius of curvature at any given point, $E_s I_s$ is the flexural rigidity of the substrate, E_s being the modulus and I_s the moment of inertia. The value of I_s can be calculated from t_s and b, the thickness and width of the substrate, respectively, by the following equation:

$$I_s = {}^1/_{12} b t_s^3 \tag{2}$$

The published theories on peel adhesion[1-9] are all based on eq. 1 and differ from each other only in the basic assumptions used in calculating M and r. Chang[1,2] does not use assumptions (*a*) and (*f*). In his model only the substrate is Hookean, the adhesive is viscoelastic, and high bending angles are permissible in the substrate in contact with the stressed adhesive. Contrary to the geometrical model of Figure 2, according to this author the peeling force acts at the point of failure, i.e., x_m is equal to zero. The solution is approximated by series and is very complicated. All the assumptions presented above underlie Bikerman's treatment,[3] but Bikerman, like Chang, assumes x_m to be zero. Kaelble[4-6] and Inoue and Kobatake[7] do not use assumption (*h*) and distinguish between failure by shear and failure by cleavage. The results are analyzed for the case when a flexible member is stripped off a solid substrate at different angles and are unsuited for calculating the variation of force with the thickness of the adhesive layer.

In the first part of the present treatment the stress distribution and the geometry of the sample prior to failure is described. The derivation is an extension of that of Spies[8] and Jouwersma.[9] The expression derived for the interdependence of the peeling force (P) and the adhesive layer thickness (t_a) contains an additional variable which is related to the geometry of the sample. This variable is either the distance of the failure point to the force axis (x_m) or the negative slope angle of the substrate at the failure point (θ). Because of the undefined relationships among either P, t_a, and x_m, or P, t_a, and θ, the Spies-Jouwersma equation itself does not define the variation of P with t_a alone.

To be able to define the geometry of the sample, a second independent equation is derived which gives the interdependence of P, t_a and θ. The combination of this equation with the equation derived in the first part of the treatment allows the elimination of θ and defines the dependence of P on t_a. To derive this second expression, the deformation of the substrate after failure is considered using a mathematical treatment analogous to that of Kaelble[4] and Inoue and Kobatake.[7]

It should be noted that the present treatment is applied to the peeling of two flexible members. The equations derived are also applicable to the 90° stripping of a flexible member from a solid substrate if t_a, as used here, is multiplied by a factor of two.

Deformation of the Substrate Prior to Failure

The most important parameters in this treatment are E_a and E_s, the modulus of the adhesive and substrate, t_s, the thickness of the substrate, b, the width of the sample, and σ_{max}, the stress at the failure point. Only the upper half of the test sample is considered. This is justified because the sample is symmetrical. As shown in Figure 2, the x axis is taken along the undeformed adhesive-substrate interface with the origin at the failure point.

It follows from assumptions (*a*) and (*c*) that

$$y = \sigma t_a / 2E_a \tag{3}$$

where y is the elongation of the adhesive and σ is the stress at any given point. The variation of y with x describes the shape of the adhesive-substrate interface.

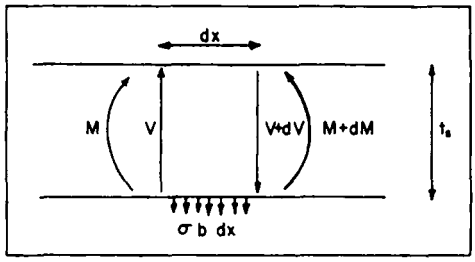

Fig. 3. Stresses and bending moments in the substrate in contact with the adhesive prior to failure. M is the bending moment, V is the shearing force, and σbdx is the force acting upon element dx.

The radius of curvature is given by the following equation.

$$1/r = y''/[1 + (y')^2]^{1.5} \sim y'' \tag{4}$$

By assumption (*f*) the first deriviative is low and be neglected. The combination of eqs. (1) and (4) gives:

$$M = E_s I_s y'' \tag{5}$$

To obtain an expression for the dependence of M on σ, the stresses in the bent substrate have to be considered as shown in Figure 3. It follows from this diagram and eq. (3) that

$$\sigma b dx = -dV \tag{6a}$$

$$V dx = dM \tag{6b}$$

$$M'' = d^2M/dx^2 = dV/dx = -b\sigma = -(2E_a b/t_a)y \tag{6c}$$

where V is the shearing force in the substrate.

By combining eqs. (2), (5), and (6c) we obtain:

$$E_s I_s y'''' = (1/12) E_s b t_s^3 y'''' = -2(E_a b/t_a)y \tag{7a}$$

$$y'''' = -(4/c^4)y \tag{7b}$$

$$c = (E_s/6E_a)^{0.25} t_s^{0.75} t_a^{0.25} \tag{7c}$$

The solution of eq. (7b) is

$$y = \exp\{-x/c\}\,[K_1 \sin(x/c) + K_2 \cos(x/c)] + \exp\{x/c\}\,[K_3 \sin(x/c) + K_4 \cos(x/c)] \tag{7d}$$

where the K's are integration constants. The boundary conditions are:

$$y_{(x=0)} = y_{max}$$

$$y''_{(x=0)} = Px_m/E_sI_s$$

$$y_{(x=\infty)} = y'_{(x=\infty)} = 0$$

The second boundary condition follows from eq. (5) and from the fact that the bending moment at the point of failure is Px_m. The final solution is most conveniently expressed in terms of σ by substituting from eqs. (3) and (7c) to obtain the stress distribution in the adhesive.

$$\sigma = \sigma_{max} \exp \{-x/c\} [\cos (x/c) - (2Px_m/\sigma_{max}bc^2) \sin (x/c)] \quad (8)$$

It may be convenient to express σ_{max} in terms of P, c, and x_m. Since the forces in the vertical direction are in balance, it follows that

$$P = b \int_0^\infty \sigma dx \quad (9)$$

The result of this integration can be presented in the following form:

$$\sigma_{max} = 2P/bc + 2Px_m/bc^2 \quad (10)$$

By substituting eq. (10) into the second term in eq. (8) we obtain:

$$\sigma/\sigma_{max} = y/y_{max} = \exp \{-x/c\} \{\cos (x/c) - [x_m/(x_m + c)] \sin (x/c)\} \quad (11)$$

The last two formulas are the Spies-Jouwersma equations. Equation (11) predicts that the adhesive is under tension for a distance $x = x_s$ (cf. Fig. 2) and is under compression for the distance x spanning between x_s and $(x_s + \pi c)$. The value of x_s is given below:

$$x_s = c \tan^{-1} [1 + (c/x_m)] \quad (12)$$

The cycles of extension and compression at $x > (x_s + \pi c)$ will be disregarded in future discussions since the value of σ in this region can be expected to be negligibly small.

The adhesive is extended by $2y_{max}$ at the point of failure, the strain at this point being $2y_{max}/t_a$. If R is the length of sample stripped per minute, x_s/R is the time needed to reach the maximum strain from the unstrained position. The rate of strain in the adhesive can be approximated by the following relation:

$$\text{rate of strain} \sim \frac{2y_{max}R}{t_a x_s} = \frac{\sigma_{max}R}{E_a x_s} \quad (13)$$

For establishing the value of x_m, the slope angle θ of y at $x = 0$ will be required (cf. Fig. 2). This can be calculated by differentiating eq. (11).

$$\tan \theta = -y'_{(x=0)} = \frac{y_{max}(2x_m + c)}{c(x_m + c)} \quad (14a)$$

Substitution from eqs. (3), (7c), and (10) gives:

$$\tan\theta = \frac{1.565\,\sigma_{max}t_a^{0.75}}{E_a^{0.75}E_s^{0.25}t_s^{0.75}} - \frac{2.449\,Pt_a^{0.5}}{bE_a^{0.5}E_s^{0.5}t_s^{1.5}} \tag{14b}$$

Deformation of the Substrate after Failure

We are considering the case where the substrate at the point of failure is at angle θ to the negative end of the symmetry axis, as shown in Figure 2. The slope angle at any given point is $(\pi - \omega)$ and the distance of any given point on the substrate from the force axis is m. The inverse radius of curvature at any given point is

$$1/r = d(\pi - \omega)/ds = -d\omega/ds \tag{15}$$

where ds is the length of an infinitesimal segment of the substrate. We can also introduce the following relationship:

$$dm/ds = \cos\omega \tag{16}$$

Since the bending moment at any given point is Pm, we can substitute from eqs. (1), (15), and (16) to obtain

$$Pm = -E_sI_s d\omega/ds = -E_sI_s(d\omega/dm)(dm/ds)$$

$$= -E_sI_s\cos\omega(d\omega/dm) \tag{17a}$$

$$P\int_0^{x_m} m dm = -E_sI_s\int_{\pi/2}^{\theta}\cos\omega d\omega \tag{17b}$$

$$x_m = \sqrt{(2E_sI_s/P)(1-\sin\theta)} \tag{17c}$$

As will be shown below, $\sin\theta$ has a low value when t_a is small. By assuming $\sin\theta$ to be zero, E_s can be calculated from the data of Table I with $t_a < 10\mu$. The calculated values are between 3×10^9 and 2×10^{10} dyne/cm.^{2}. As can be seen from the data of Table II, these values are of the right order of magnitude, indicating that eq. (17c) gives the correct physical picture.

TABLE II

Modulus of Cellophane Calculated from the Stress-Strain Curve at 12.5%/min. Elongation Rate

Method of calculation	Modulus (dyne/cm.^{2} $\times .10^{-8}$)[a]
Initial slope	104
Stress/strain ratio at 0.05 strain	32
0.10	20
0.20	12.5
break	7.4
Slope at strains >0.1	4.8

[a] Stress divided by strain where the strain is measured as length fraction, not as per cent.

By combining eq. (17c) with eqs. (7c) and (10) x_m can be eliminated:

$$\sigma_{max} = \frac{3.13\ E_a^{0.25}}{bE_s^{0.25}t_a^{0.75}} \frac{P}{t_s^{0.25}} + \sqrt{\frac{4E_a}{b}} \sqrt{\frac{P}{t}(1 - \sin\theta)} \tag{18}$$

The Variation of the Peeling Force with the Thickness of the Adhesive Layer

In eqs. (14b) and (18) we have two independent expressions containing P, t_a, and θ as variables and σ_{max}, E_a, E_s, t_s, and b as parameters. These two equations could be combined into a single expression to eliminate the variable θ but for purposes of calculations it is convenient to work with two separate equations. For the treatment of the data it is useful to define two new parameters, α and β, which are independent of P and t_a.

$$\alpha = b\sigma_{max}c/2t_a^{0.25} = 0.319b\sigma_{max}E_s^{0.25}E_a^{-0.25}t_s^{0.75} \tag{19}$$

$$\beta = 2E_sI_st_a^{0.5}/c^2 = 0.409bE_s^{0.5}E_a^{0.5}t_s^{1.5} \tag{20}$$

By substituting these parameters into eqs. (18) and (14b), respectively, one obtains:

$$P/t_a^{0.25} = \alpha - \sqrt{\beta}\sqrt{(P/t_a)(1 - \sin\theta)} \tag{21}$$

$$\tan\theta = (2\alpha/\beta)t_a^{0.75} - (1/\beta)Pt_a^{0.5} \tag{22}$$

Strictly speaking, these equations should apply only to small deflections in the substrate prior to failure, that is, for low values of θ, because of the assumptions made in eq. (5). However, as will be shown below, the experimental data fit these equations well over the whole range of θ values. This justifies the discussion of the implications of these equations without putting restrictions on their validity.

It follows from eq. (21) that $P/t_a^{0.25}$ can never exceed α. A consequence of this is that $\tan\theta$ must monotonically increase with t_a according to eq. (22) and at high t_a values θ approaches $\pi/2$. Thus at high t_a values $(1 - \sin\theta)$ approaches zero and eq. (21) reduces to

$$P = \alpha t_a^{0.25} \tag{23}$$

As already indicated, Bikerman[3] solved eq. (7b) for the boundary condition $x_m = 0$. He derived an equation identical to eq. (23) except for a factor of $2^{0.25}$. This factor is due to the fact that the present derivation concerns the peeling of two flexible substrates, whereas Bikerman considered the case involving a flexible and a rigid substrate. The present analysis shows that Bikerman's equation is a limiting case applicable only for situations leading to high θ or low x_m values.

Another limiting case is at low t_a values when $\tan\theta$ and $\sin\theta$ approach zero. Here the following relation should hold:

$$\alpha = P/t_a^{0.25} + \beta^{0.5}(P/t_a)^{0.5} \tag{24}$$

This relation shows that with increasing $P/t_a^{0.25}$ the value of P/t_a must decrease. It follows that the log-log plot of P vs. t_a can have limiting slopes of 1 and 0.25, and that over a small range of t_a values P may be proportional to powers of t_a with power coefficients between 1 and 0.25. This prediction is consistent with Bikerman's data,[10] showing that over a limited range of adhesive layer thickness P was proportional to $t_a^{0.5}$.

APPLICATION OF THE THEORY TO THE RATE INDEPENDENT ADHESIVE FAILURE DATA

Experimental Results

The experiments were carried out as described in Part I. The dependence of mean peeling force values upon t_a is shown in Figure 4. It is evident that these log-log plots are concave towards the thickness axis and have slope values within the theoretical limits.

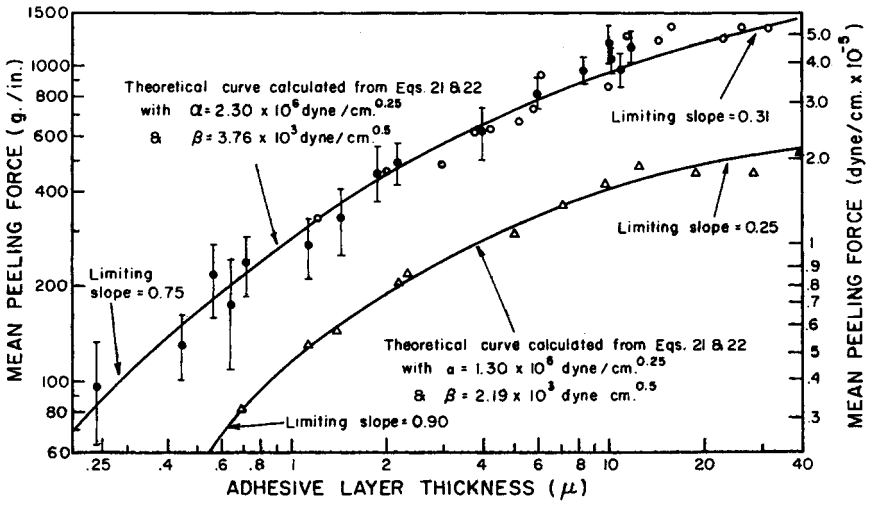

Fig. 4. The variation of peeling force with adhesive layer thickness when rate-independing adhesive failure occurs at 2 to 20 in./min. cross-head speeds. (O, ●) Rhoplex HA-8 from two different experimental series with two identical but separately prepared batches. The half length of the bars is the standard deviation determined from probability charts, as explained in Part I. The standard deviation of the mean values should be lower than indicated here. (△) Polymer 305-A.

In Part I it was demonstrated that the steady-state peeling force at a given rate and adhesive layer thickness oscillates randomly when Rhoplex HA-8 or Polymer 305-A binders are used. A technique is also described by which the standard deviation of the steady-state force values, as recorded on the Instron chart, can be determined. Some of these standard deviation values are indicated by vertical bars in Figure 4. It is striking that the ratio between the standard deviation and the mean force value

decreases with increasing adhesive layer thickness. This observation can be readily explained in terms of the theory.

The variability in the peeling force when a given sample is tested can be caused by two types of imperfections in the sample: variation in t_a arising from imperfections at coating of the cellophane and variation in the adhesive strength, as measured by α, due to imperfect annealing. At low t_a values, when $P/t_a^{0.25}$ is low and sin θ is almost zero, P would be in the first approximation proportional to α^2 and to t_a [cf. eq. (24)]. At high t_a values, when $P/t_a^{0.25}$ is high and sin θ almost unity, P would be approximately proportional to α and $t_a^{0.25}$ [cf. eq. (23)]. It can be readily seen that imperfections in the sample must have a much larger effect on the peeling force at low t_a values than at high.

Determination of the Parameters α and β from Peel Test Data

By substituting the P and t_a data, such as those of Figure 4, into eqs. (21) and (22), the parameters α and β can be easily determined by trial and error. The value of tan θ is calculated for each pair of P and t_a values according to eq. (22) using assumed values of α and β. If the parameters are selected correctly, the points of the plot of $P/t_a^{0.25}$ against $(P/t)^{0.5}$ $(1 - \sin\theta)^{0.5}$ should fall on a straight line with an intercept of α and a slope of $-\beta^{0.5}$. Under such conditions the order of magnitude of α can be estimated from the high P and t_a values according to eq. (23), and the order of magnitude of β can be estimated from eq. (24) based on low P and t_a values.

In the present work the Bendix G-15D computer was used and Eqs. (21) and (22) were solved for α and β so that the sum square of the difference between $P/t_a^{0.25}$ and $[\alpha - \beta^{0.5}(P/t_a)^{0.5}(1 - \sin\theta)^{0.5}]$ was minimized. The data of Figure 4 gave the values shown in Table III.

TABLE III
Data from Figure 4

Binder	Parameter	Mean value	Coefficient of variation = standard dev./mean value, %
Rhoplex HA-8	α	2.30×10^6 dyne/cm$^{0.25}$	4
	$\beta^{0.5}$	61.3 dyne$^{0.5}$ cm$^{0.25}$	18
	β	3.76×10^3 dyne cm$^{0.5}$	36
Polymer 305-A	α	1.30×10^6 dyne/cm$^{0.25}$	25
	$\beta^{0.5}$	46.8 dyne$^{0.5}$ cm$^{0.25}$	14
	β	2.19×10^3 dyne cm$^{0.5}$	28

It should be noted that E_a is proportional to β^2. If E_s, b, and t_s were known accurately, the coefficient of variation in the estimated value of E_a would be the coefficient of variation in β^2, which is 85% for Rhoplex

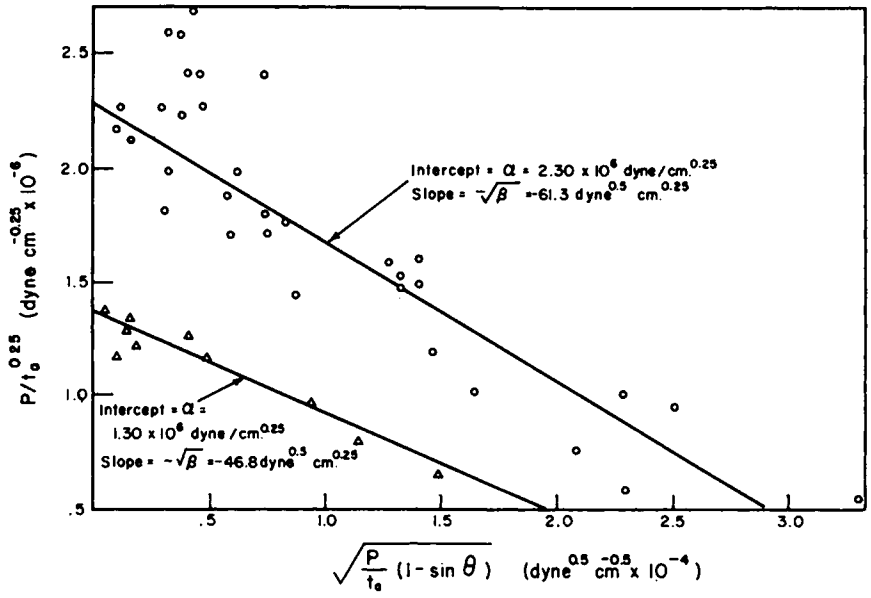

Fig. 5. Plot of the experimental data of Fig. 4 according to eqs. (21) and (22). (O) Rhoplex HA-8. (Δ) Polymer 305-A.

HA-8 and 63% for Polymer 305-A. This means that E_a can be established only with very poor accuracy from the present data. As to σ_{max}, this is proportional to $\alpha\beta^{0.5}$ which has a coefficient of variation 23% for Rhoplex HA-8 and 50% for Polymer 305-A.

Using these α and β values, the data of Figure 4 are plotted according to eq. (21) in Figure 5. The correlation coefficients of these plots are significant over the 99% probability level. The dependence of P on t_a was also calculated and the corresponding theoretical curves are drawn into Figure 4. As can be seen, these curves follow very closely the experimental points. The standard deviations of the experimental points from the theoretical curves as 3.85×10^4 dyne/cm. for Rhoplex HA-8 and 1.70×10^4 dyne/cm. for Polymer 305-A.

Estimation of E_s, E_a, and σ_{max}

As shown above, the theory predicts correctly the variation of P with t_a. The ultimate test for the validity of the theory is to calculate E_s, E_a, and σ_{max} from α and β and see whether these values are of a reasonable order of magnitude. Here we encounter two problems. First, the modulus of the unsupported cellophane and the modulus and cohesive strength of free acrylic films can depend on the rate of testing and the elongation. This means that it is necessary to estimate the rate of deformation and the maximum deformation in the peel test to be able to select independently determined modulus values for the cellophane and the binder which should match the values calculated from α and β. The second problem is that only two

of the five parameters in α and β, b and t_s, can be determined accurately by independent methods. To be able to calculate E_a and σ_{max}, the value for E_s has to be assumed. However, if the value of E_s is once fixed, E_a and σ_{max} are completely defined by α and β.

To form a rough estimate concerning the deformation of the cellophane in the peel test, it is assumed that it forms a quarter circle with the neutral axis at the center of the cellophane having a radius equal to $(x_m + x_s)$. This assumption is quite reasonable since the data of Figure 7 show that $(x_m + x_s)$ is of the same order of magnitude as the radius of curvature of the cellophane at the breaking point. The average elongation e_s along the half thickness under tension is given below.

$$e_s = 0.25t_s/(x_m + x_s) \tag{25}$$

Furthermore it is assumed that the length of the deformed cellophane is $(x_m + x_s)\pi/2$ and that undeformed cellophane has to travel the distance $(x_m + x_s)\pi/4$ before it is subject to an elongation equal to e_s. If R is the length of sample peeled per minute,

$$\tau = (x_m + x_s)\pi/4R \tag{26}$$

is the time needed to obtain e_s elongation and the rate of deformation is

$$e_s/\tau = Rt_s/\pi(x_m + x_s)^2 \tag{27}$$

Two adhesive layer thickness values in the middle of the range of the experimental t_a values, 1 and 10 μ, were selected. Using the α and β values obtained for Rhoplex HA-8 and assumed values of E_s in the range of 2.5 $\times 10^8$ to 2.5 $\times 10^9$ dyne/cm.^{2}, E_a, P, θ, x_m, x_s, e_s, and τ have been calculated. The value of e_s was found to range between 5 and 20%. The rate of elonga-

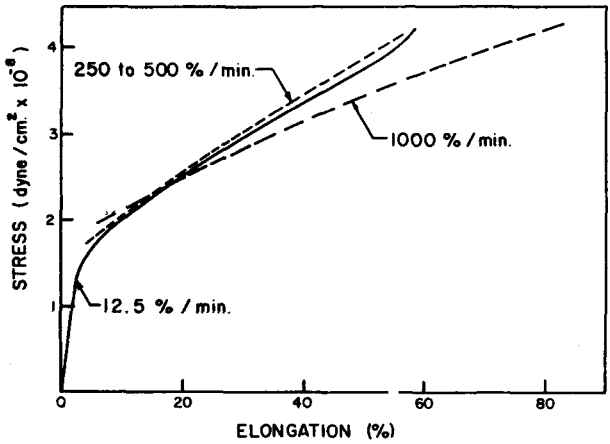

Fig. 6. Cellophane stress–strain curves at different elongation rates. The fact that the curve corresponding to 1000%/min. has a relatively low slope is probably due to jaw error.

tion was in the range of 1×10^4 to 1.5×10^5%/min. when R was assumed to be 5 cm./min.

The stress-strain curves of cellophane are presented in Figure 6. The data suggest that these curves are insensitive to rate of strain in the 12.5 to 500%/min. range. As the rate of strain is increased to 1000%/min., the slope of the curves is reduced probably due to jaw error. It was, of course, not possible to determine the stress-strain properties of the cellophane in the 10^4 to 10^5%/min. range to obtain results which would be rigorously applicable to the peel test. Since the stress-strain curves did not change over a rather wide range of straining rates, we can make the assumption that the 12.5%/min. curve is valid for any straining rate although this assumption is admittedly tenuous. If this is so, the effective modulus of the cellophane depends less on the straining rate than on the maximum deformation, e_s. Table II gives a few modulus values calculated from the 12.5%/min. stress-strain curve. If the previous estimate of the maximum elongation is correct and if the modulus varies with increasing straining of the volume elements in bending as in tensional deformation, then the effective cellophane modulus in peeling should be in the range of 1.25 to 3.2×10^9 dyne/cm.^{2}.

TABLE IV
Stress-Strain Properties of Free Rhoplex HA-8 Films

Rate of elongation (%/min)	Initial modulus (dyne/cm.^{2} $\times$ 10^{-6})	Breaking elongation (%)	Ultimate stress[a] (dyne/cm.^{2} $\times$ 10^{-7})	Breaking modulus[a] (dyne/cm.^{2} $\times$ 10^{-6})
4000	5.50	680	1.90	2.80
2000	5.03	690	1.55	2.25
1000	4.10	790	1.27	2.70
400	2.55	670	1.08	1.60
200	1.75	630	0.87	1.37
100	2.33	580	0.62	1.06
40	1.85	550	0.53	0.97

[a] The stress-strain curves were concave towards the strain axis. The initial modulus was determined from the initial slope. The breaking modulus is the ratio between ultimate stress and breaking strain, where the strain is measured as length fraction, not as per cent.

The stress-strain properties of the two binders were determined as described in Part I and are shown in Tables IV and V. With increasing rate of strain the ultimate strength and modulus of Rhoplex HA-8 increases appreciably. Polymer 305-A exhibits cold flow at low rates of strain but breaks clearly at high rates. In these measurements up to 4000%/min. elongation rates were employed. As will be shown later, the effective elongation rates of the binder at the peel test is in 10^5 to 10^6%/min. range. If the demonostrated trends in the polymer properties continue as the straining rates are increased to such high levels, we would expect that the effec-

TABLE V
Stress-Strain Properties of Free Polymer 305-A Films[a]

Rate of elongation (%/min.)	Stress (dyne/cm.^{2} $\times 10^{-7}$)		Elongation (%)		Modulus[b] (dyne/cm.^{2} $\times 10^{-6}$)	
	At max. of stress-strain curve	At break	At max. of stress-strain curve	At break	Initial	At break
4000	—	1.03	—	1880	4.5	0.69
400	0.41	—	~200	—	8.2	—
40	0.20	—	~120	—	5.9	—

[a] At 400 and 40%/min. elongation rate the specimens did not break but exhibited cold flow at a constant stress.

[b] Stress divided by strain. The strain measured as length fraction, not as per cent. The initial modulus was calculated from the initial slope of the stress-strain curve.

tive ultimate strength and modulus of the binders in peeling will be higher than measured at 4000%/min. elongation rate.

As shown in Part I, the failure reverts from cohesive to adhesive as the peeling rate is increased. We would thus expect that σ_{max} should be of the same order of magnitude as the ultimate breaking stress of the binder but should be higher than this value at 4000%/min. elongation. As to E_a, it should have an effective value of the same order of magnitude as the modulus-at-break, since at adhesive-failure-peeling the binder is strained close to the point where it would fail cohesively.

To see whether the experimental α and β values are of the right order of magnitude, we can estimate these values independently by setting $E_s = 2 \times 10^9$ dyne/cm.^{2}, E_a equal to the 4000%/min. breaking modulus of the binder, and σ_{max} equal to three times the 4000%/min. ultimate stress of the binder. The values calculated in this way are compared with the experimental values in Table VI. These comparisons show that the experimental α and β values are definitely of the right order of magnitude.

TABLE VI
Values of α and β

	Rhoplex HA-8		Polymer 305-A	
	Experimental	Estimated	Experimental	Estimated
α (dyne/cm$^{0.25}$ $\times 10^{-6}$)	2.30	1.51	1.30	1.60
β(dyne cm$^{0.5}$ $\times 10^{-3}$)	3.76	8.75	2.19	4.33

It was already pointed out that for calculating σ_{max} from α and β, E_s has to be assumed. Using the experimental α and β values of Rhoplex HA-8, σ_{max} and E_a were calculated with the aid of different E_s values and the results are shown in Table VII. It is evident that the magnitude of the calculated σ_{max} and E_a values depends on the magnitude of the assumed

E_s. However, this is not bad if the purpose of testing is not to establish the absolute value of σ_{max} accurately but rather to compare the σ_{max} values of different adhesives using the same substrate. In this case it is convenient to assume an arbitrary value of E_s within the probable range of values, and calculate σ_{max} and E_a with this single value. Any error in the estimated E_s value will introduce an error into the calculated value of σ_{max} and E_a which is in the same direction and of the same order of magnitude for all adhesives and will have no effect on the validity of the comparison.

It may be convenient to select $E_s = 5 \times 10^8$ dyne/cm.^{2} in the present system because E_a calculated with the aid of this value is very close to the breaking modulus of Rhoplex HA-8 at 4000%/min. extension rate, the calculated and experimental values being 2.47 and 2.80 $\times 10^6$ dyne/cm.^{2} The calculated E_a of Polymer 305-A is 8.4 $\times 10^5$ dyne/cm.^{2} when the same E_s value is used, and this E_a is close to the 4000%/min. breaking modulus, 6.9 $\times 10^5$ dyne/cm.^{2}. The thus calculated σ_{max} values, 1.24 $\times 10^8$ and 5.1 $\times 10^7$ dyne/cm.^{2} for Rhoplex HA-8 and Polymer 305-A, respectively, are about 5 or 6 times higher than the ultimate strength of these polymers at 4000%/min. extension.

LIMITATIONS AND IMPLICATIONS OF THE THEORY

Geometrical Parameters

With the values of α and β known and E_s assumed to be 5 $\times 10^8$ dyne/cm^2., the system is completely defined and the variation of the force, geometry, and the rate of strain in the adhesive and substrate can be calculated from the equations presented above.

The variation of the most important geometrical parameters with Rhoplex HA-8 adhesive layer thickness is presented in Figure 7. It should be noted that if any of these parameters could be independently determined E_s would be defined by the system and would not have to be assumed. Unfortunately the order of magnitude of x_m, x_s, and r_0 is in the 10^{-3} to 10^{-2} cm. range and it would require pictures of 100 to 1000-fold magnification to be able to determine these parameters with meaningful accuracy. Such pictures on a fast moving system, as the present one, would be difficult to prepare.

Over the experimental range of t_a values x_s increases about 6 fold, while P increases 20 fold. Intuitively one would expect that the main reason for the fact that P increases with t_a is that x_s also increases with t_a. In the first approximation this is true, but P increases faster than x_s because, as will be shown later, at low t_a values large proportions of the total force is used for compressing the sample in the region between x_s and $(x_s + \pi c)$.

The radius of curvature at the breaking point (r_0) passes through a minimum with increasing thickness because the bending moment acting on the cellophane at the breaking point, Px_m, passes through a maximum.

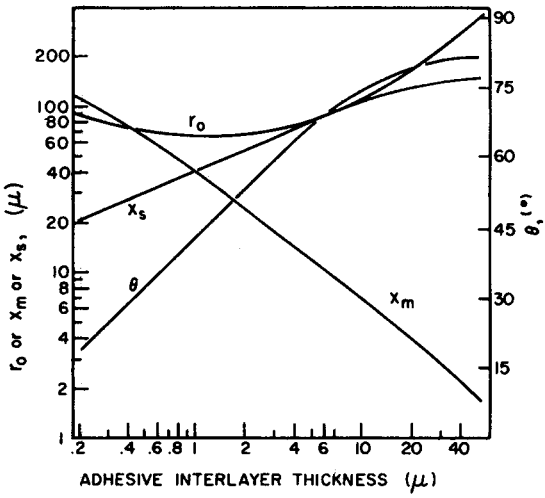

Fig. 7. Calculated geometrical parameters corresponding to the Rhoplex HA-8 theoretical curve of Fig. 4 with the modulus of the cellophane assumed to be 5×10^8 dyne/cm.^{2}. The symbol r_0 is the radius of curvature of the cellophane at the failure point, x_m is the distance of the failure point from the force axis, x_s is the length of the adhesive layer which is under tension, and θ is the negative slope angle of the cellophane at the failure point. The cellophane is 40.5 μ thick.

The most important curve in Figure 7 shows the variation of θ with t_a. As can be seen, the calculated θ assumes high values as the adhesive layer thickness is increased. This suggests that there is an inconsistency between the assumed model and the picture it gives when applied to actual data, since in eq. (4) it is assumed that the slope angle is small. However, this assumption and the neglecting of $(y')^2$ relative to unity in eq. (4) does not interfere seriously with the calculations as long as θ is less than 45°. When the term $(y')^2$ is neglected, r in eq. (4) is underestimated and it follows from the geometrical model (cf. Fig. 2) that underestimation of r causes overestimation of θ in the theory. Thus the effective experimental θ is lower than the calculated value. Furthermore, comparison of the photographs represented by Figure 1 and of the model of Figure 2 reveals that θ cannot be accurately defined for the actual experiment. It follows that the calculated value of θ cannot be used for assessing the validity of the theory.

The exponentially damped wave function describing the dependence of y on x by eq. (11) may give about the correct qualitative picture of the shape of the adhesive-substrate interface and fitting the data to this equation probably partially compensates for the errors in the model. This may explain why the rheological parameters derived from Eqs. (21) and (22) are of the right order of magnitude.

Rate of Strain in the Adhesive and Substrate

The data of Tables IV and V show that the rheological properties of the adhesive in the present system are strongly dependent on the rate of strain-

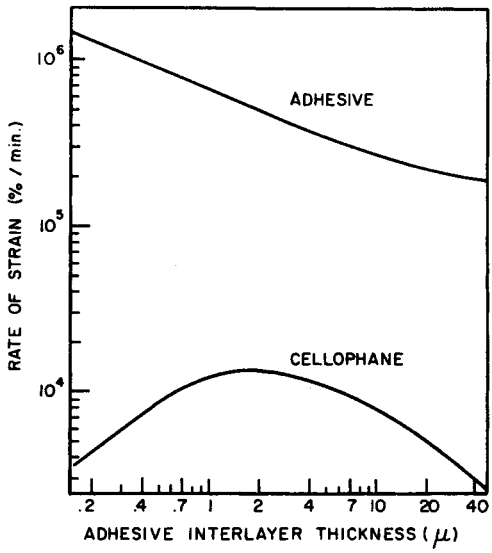

Fig. 8. Estimated rate of strain in the Rhoplex HA-8 containing samples of Fig 4. at 5 in./min. cross-head speed when the modulus of the cellophane is assumed to be 5×10^8 dyne/cm.^{2}.

ing. In the model, however, the modulus values were assumed to be rate independent and the question arises how serious an error was introduced by this approximation.

Figure 8 shows the variation of the calculated straining rate with the thickness of the adhesive layer at 5 in./min. cross-head speed. If these data are approximately correct, the straining rate in the adhesive is about 10^5 to 10^6%/min. and decreases by a factor of 6 over the experimental range of adhesive layer thickness. It is probable that at these very high rates of strain no viscous deformation takes place and the modulus is relatively insensitive to a 6-fold change in straining rate. The fact that the peeling force in adhesive failure in independent of the cross-head speed also supports this argument. Thus the Hookean approximation is justifiable.

The same arguments also hold for the substrate properties. The straining rate of the substrate has the order of magnitude of 10^4%/min. It passes through a maximum with increasing interlayer thickness and an average value over the whole range of adhesive layer thicknesses should be a well-defined representative figure.

The Effect of Adhesive Layer in Contact with the Substrate upon the Flexural Rigidity of the Substrate

After failure occurs, fragments of the adhesive remain on each of the two substrate films. Furthermore, in the present experiments the substrate was coated on both sides prior to annealing so that there was adhesive on the two surfaces of the sandwich. These adhesive layers could increase

TABLE VII

Dependence of E_a and σ_{max} upon the Assumed Value of E_s when $\alpha = 2.30 \times 10^6$ dyne/cm.$^{0.25}$ and $\beta = 3.76 \times 10^3$ dyne cm.$^{0.5}$

E_s (dyne/cm.^{2} $\times 10^{-8}$)	22.5	20	17.5	15	12.5	10	7.5	5	2.5
E_a (dyne/cm.^{2} $\times 10^{-6}$)	0.55	0.62	0.71	0.82	0.97	1.23	1.65	2.47	4.94
σ_{max} (dyne/cm.^{2} $\times 10^{-7}$)	5.56	5.88	6.30	6.81	7.43	8.39	9.61	12.35	16.72

the flexural rigidity of the substrate and the question arises how big an error is introduced by this effect.

To answer this question, we have to calculate the flexural rigidity of a two component laminate composed of layers of t_s and t_a thickness having E_s and E_a modulus. This problem has been treated by Inoue and Kobatake.[7] If $E_{sa}I_{sa}$ is the flexural rigidity of the laminate, and $v = E_a/E_s$ and $w = t_a/t_s$, the following relationship holds:

$$\frac{E_{sa}I_{sa}}{E_sI_s} = \frac{(1 - vw^2)^3(1 - v) + [vw(v + 2) + 1]^3 + v(vw^2 + 2w + 1)^3}{2(1 + vw)^3} \quad (28)$$

In the present experiments v is about 0.005 and w is at most 1. It follows that the error in the flexural rigidity due to the binder sticking to the substrate is at most 4% and negligible. However, in other systems this type of error may be considerable.

The Compressive and Tensional Stresses in the Glue Line

The fact that when a sample is peeled there are compressive stresses prior to the development of tensional stresses is a well-known phenomenon.[11] For the data of Figure 4 the compressive force can be calculated. The total peeling force P can be broken down into two components, P_{ten} and P_{comp}, the tensional and compressive force:

$$P = P_{ten} - P_{comp} \quad (29a)$$

$$P_{ten} = b \int_0^{x_s} \sigma dx \quad (29b)$$

$$P_{comp} = -b \int_{x_s}^{\infty} \sigma dx \quad (29c)$$

By substituting from eq. (11), integrating and substituting from eqs. (9) and (12), we obtain:

$$P_{comp} = b\,\sigma_{max}\,c \exp\{-x_s/c\} \cos(x_s/c)\,[1 + (c/x_m)^2/2(1 + c/x_m)] \quad (30a)$$

$$P_{comp} = b\,\sigma_{max}\,c \exp\{-x_s/c\}\,[\cos(x_s/c) + (\sqrt{1 - \cos^2(x_s/c)} - 1)^2/2 \sqrt{1 - \cos^2 x_s/c}] \quad (30b)$$

Since both c/x_m and x_s/c increase with t_a, there are terms in eq. (30b) which decrease and others which increase with increasing t_a. Due to this self-

compensation, P_{comp} is insensitive to variation in t_a. When Rhoplex HA-8 parameters are substituted in this formula and if $b = 1$ cm, P_{comp} increases from 8.30×10^4 dyne to 1.27×10^5 dyne at t_a values between 0.2 to 40 μ. Since the peeling force in this t_a range varies between 2.76×10^4 and 5.64×10^5 dyne/cm., it follows that at very low thicknesses the absolute value of the compresssive force is higher than the measured peeling force.

On intuitive grounds we predicted that the main reason for an increment in the peeling force is that x_s increases with the interlayer thickness. Now that it is shown that the tensional force is the sum of the measured force and the compressive force, it is of interest to see how P_{ten} varies with x_s. The Rhoplex HA-8 data suggest that at t_a values between 0.2 and 40 μ P_{ten} is almost proportional to x_s. In this range of t_a values the following relation holds for a 1-cm. wide sample when x_s is measured in cm. and P in dyne:

$$P_{ten} = 3.5 \times 10^7 x_s^{0.95}$$

It should be noted that according to eq. (12), x_s approaches the value of $(\pi/2)c$ at very high t_a values. At very high t_a values P itself becomes proportional to c. [cf. eqs. (7c) and (23)]. It follows from eqs. (29a) and (30b) that at high t_a values the following relation holds:

$$P_{ten} = (b\sigma_{max}/\pi)[1 + \exp\{-\pi/2\}]x_s$$

By substituting 1 cm. for b and 1.24×10^8 dyne/cm.^{2}, for σ_{max} one obtains:

$$P_{ten} = 4.6 \times 10^7 x_s$$

Since this relationship is not too dissimilar from the one that holds for low to intermediate t_a values, it can be concluded that the average tensional stress P_{ten}/bx_s varies very little as the thickness of the adhesive layer is increased.

The advice of Drs. R. H. Shoulberg, S. Gratch, and R. Steele was invaluable. The calculations on the computer were carried out by Mr. L. DeFonso.

Glossary of Symbols

Symbol	Unit	Definition
b	cm.	Width of sample
c	cm.	Parameter, $c = (E_s t_a / 6E_a)^{0.25} t_s^{0.75}$
e_s	—	Maximum fractional elongation in substrate
E_a	dyne/cm.^{2}	Modulus of adhesive
E_s	dyne/cm.^{2}	Modulus of substrate
F	g./in. or dyne/cm.	Peeling force per unit width
I_s	cm.^{4}	Moment of inertia of substrate
m	cm.	Distance of any given point on substrate from the axis of the peeling force

Glossary of Symbols (*continued*)

Symbol	Unit	Definition
M	dyne cm.	Bending moment
P	dyne	Peeling force
P_{comp}	dyne	Compressive force acting on sample
P_{ten}	dyne	Tensional force acting on sample
s	cm.	Length of substrate
t_a	cm. or μ	Thickness of the adhesive layer
t_s	cm. or μ	Thickness of the substrate
r	cm.	Radius of curvature of substrate
r_0	cm.	Radius of curvature of substrate at the point of failure
R	cm/min.	Rate of peeling
v	—	$v = E_a/E_s$
V	dyne	Shearing force in substrate
w	—	$w = t_a/t_s$
x	cm	Distance parallel to the symmetry axis of the sample
x_m	cm.	Distance of the failure point from the force axis
x_s	cm.	Length of glue line under tension
y	cm.	Elongation of the adhesive prior to failure
y_{max}	cm.	Elongation of the adhesive at failure
α	dyne/cm$^{0.25}$	Parameter, $\alpha = 0.319b\sigma_{max}[E_s/E_a)^{0.25} t_s^{0.75}$
β	dyne cm.$^{0.5}$	Parameter, $\beta = 0.409bE_s^{0.5}E_a^{0.5}t_s^{1.5}$
ω	degree or radian	Negative slope angle of substrate
σ	dyne/cm.^{2}	Stress in the adhesive layer
σ_{max}	dyne/cm.^{2} or psi	Stress in the adhesive layer at failure
τ	min.	Time needed for developing maximum curvature in substrate
θ	degree or radian	Negative slope angle of substrate at the point of failure

References

1. Chang, F. S. C., *J. Appl. Phys.*, **30**, 1839 (1959).
2. Chang, F. S. C., *Trans. Soc. Rheology*, **4**, 75 (1960).
3. Bikerman, J. J., *J. Appl. Phys.*, **28**, 1484 (1957).
4. Kaelble, D. H., *Trans. Soc. Rheology*, **3**, 161 (1959).
5. Kaelble, D. H., *Trans. Soc. Rheology*, **4**, 45 (1960).
6. Kaelble, D. H., *Adhesive Age*, May, 1960.
7. Inoue, Y., and Y. Kobatake, *Appl. Sci. Res., Sec.* **A8**, 321 (1959).
8. Spies, G. J., *Aircraft Eng.*, **25**, 64 (1953).
9. Jouwersma, C., *J. Polymer Sci.*, **45**, 253 (1960).
10. Bikerman, J. J., *J. Appl. Polymer Sci.*, **2**, 216 (1959).
11. DeBruyne, N. A., *Nature*, **180**, 262 (1957).

Synopsis

The purpose of this analysis is to find a method of calculating the maximum stress at failure from the variation of the peel force with the thickness of the adhesive layer If

the failure is in the binder/substrate interface, this maximum stress is the adhesive bond strength. In the model it is assumed that, among other things, both substrate and adhesive are Hookean, the stresses parallel to the symmetry axis of the sample and the shear stresses are negligible, and the deflection of the substrate prior to failure is small. The latter assumptions are very questionable but the assumption involving Hookean behavior is a good approximation. It is shown that the rate of deformation in the sample is in the 10^4 to 10^6%/min. range. At such high rates of deformation viscoelastic bodies are expected to approach Hookean behavior. Two separate equations are derived describing the variation of the peeling force with adhesive layer thickness. These equations also contain an additional variable, the slope angle of the substrate at the failure point. This variable can be eliminated by combining the two equations. The parameters in the final expressions are the moduli of the binder and substrate, thickness of the binder, width of the sample, and the maximum stress at the failure point. The theoretical analysis also defines the geometry of the sample and allows the estimation of the rate of strain in the adhesive and in the substrate. Furthermore, it predicts the existence of compressive stresses which develop prior to tensional stresses. These compressive and tensional stresses in the sample can be separately calculated, and it is possible to establish the size of the area where these stresses exist at steady state conditions. The measured peeling force is proportional to the difference between the sum of tensional and the sum of compressive stresses. Data obtained with cellophane substrates and acrylic binders at high peeling rates, where the force is rate independent and the failure is adhesive, are analyzed in terms of the theory. The rheological parameters calculated from peel test data are of the right order of magnitude and the shape of force/adhesive layer thickness plot is consistent with theoretical predictions. It is also shown that the magnitude of the compressive force in the glue line changes only to a small extent with the thickness of the adhesive layer and that the tensional force in the glue line is approximately proportional to the area under tension.

Résumé

Le but de cette étude est la détermination d'une méthode de calcul de la résistance maximale à la cassure à partir de la variation de force de décollage suivant l'épaisseur de la couche adhésive. Si la cassure est localisée à l'interface substrat-liant cette résistance maximale est la force d'adhésion. Dans le modèle on suppose entr'autres que substrat et adhésif sont tous deux Hookéens que les forces sont paralèles à l'axe de symétrie de l'échantillon, que les forces de cisaillement sont négligeables et que la déformation du substrat avant rupture est petite. Si les dernières hypothèses sont discutables, celle concernant le comportement Hookéen constitue une bonne approximation. On montre que la vitesse de déformation dans l'échantillon est de l'ordre de 10^4 à 10^6%/min. Pour de telles vitesses de déformation, on peut s'attendre à ce que des corps viscoélastiques se comportent approximativement suivant le modèle Hookéen. On déduit deux équations différentes qui décrivent la variation de la force de décollage avec l'épaisseur de la couche adhésive. Ces équations contiennent aussi une variable supplémentaire: l'angle de la tangente du substrat à l'endroit de la cassure. On peut éliminer cette variable en combinant les deux équations. Les paramètres contenus dans les expressions finales sont les modules du substrat et du liant, l'épaisseur du liant, la largeur de l'échantillon et la tension maximum àl 'endroit de cassure. L'analyse théorique définit ainsi la géométrie de l'échantillon et permet d'estimer la vitesse de tension dans l'adhésif et le substrat. De plus elle prédit l'existence de forces de compression qui se développent avant les forces de tension. Ces forces de compression et de tension peuvent être calculées séparément et il est possible d'établir la grandeur du domaine à ces forces existant à l'état stationnaire. La force de décollement mesurée est proportionnelle à la différence entre la somme des forces de tension et la somme des forces de compression. On analyse au point de vue théorique des résultats obtenus avec un substrate de cellophane et des liants acryliques pour des grandes vitesses de décollement,

où la force est indépendante de la vitesse et la cassure est adhésive. Les paramètres rhéologiques calculés à partir des résultats des tests de décollage sont du bon ordre de grandeur et la forme de la courbe force/épaisseur de la couche adhésive est en accord avec les prédictions de la théorie. On montre aussi que la grandeur de la force de compression change peu avec l'épaisseur de la couche adhésive et que la force de tension est à peu près proportionnelle à la surface sous tension.

Zusammenfassung

Der Zweck der vorliegenden Untersuchung ist es, eine Methode zur Berechnung der maximalen Spannung beim Bruch aus der Abhängigkeit der Abziehkraft von der Dicke der Klebeschichte zu finden. Wenn der Bruch in der Binder-Substratgrenzfläche stattfindet, ist diese maximale Spannung zugleich die Festigkeit der Klebeverbindung. Für das Modell wird angenommen, dass Substrat und Klebemittel sich entsprechend dem Hookeschen Gesetz verhalten, die Spannungen parallel zur Symmetrieachse der Probe und die Schubspannungen vernachlässigbar sind und die Verbiegung des Substrates vor dem Bruch klein ist. Die letzteren Annahmen sind recht fragwürdig, die Annahme bezüglich des Hookeschen Verhaltens stellt aber eine gute Näherung dar. Es wird gezeigt, dass die Deformationsgeschwindigkeit in der Probe im Bereich von 10^4 bis 10^6 %/min liegt. Bei so hohen Deformationsgeschwindigkeiten kann man für viskoelastische Körper ein Hookesches Verhalten erwarten. Zwei unabhängige Gleichungen werden für die Abhängigkeit der Abziehkraft von der Dicke der Klebeschichte abgeleitet. Diese Gleichunge enthalten auch eine zusätzliche Variable, nämlich den Neigungswinkel des Substrats beim Bruch. Diese Variable kann durch Kombination der beiden Gleichungen eliminert werden. Die Parameter in den schliesslich erhaltenen Ausdrücken sind die Moduln von Binder und Substrat, die Dicke des Binders, die Breite der Probe und die maximale Spannung beim Bruch. Die theoretische Analyse legt auch die geometrischen Verhältnisse der Probe fest und gestattet die Bestimmung der Verformungsgeschwindigkeit im Klebestoff und im Substrat. Weiters lässt sie das Auftreten von Kompressionsspannungen vor den Tensionsspannungen erwarten. Diese Kompressions- und Tensionsspannungen in der Probe können getrennt berechnet werden und es ist möglich die Grösse der Fläche festzulegen, wo diese Spannungen im stationären Zustand bestehen. Die gemessene Abziehkraft ist dem Unterschied zwischen der Summe der Tensions- und der Summe der Kompressionsspannungen proportional. An Cellophan als Substrat und Acrylbindern bei hoher Abziehgeschwindigkeit, wo die Kraft geschwindigkeitsunabhängig ist und der Bruch im Klebemittel auftritt, erhaltene Ergebnisse werden einer Analyse im Lichte der Theorie unterzogen. Die aus den Abziehtestdaten berechneten rheologischen Parameter liegen in der richtigen Grössenordnung und die Gestalt des Diagramms Kraft gegen Dicke der Klebeschicht stimmt mit den theoretischen Erwartungen überein. Es wird gezeigt, dass die Grösse der Kompressionskraft in der Verleimungslinie nur wenig von der Dicke der Klebeschichte abhängt und dass die Tensionskraft in der Verleimungslinie angenähert der Fläche unter Spannung proportional ist.

Received December 4, 1961